Organic & Biomolecular Chemistry

PAPER

View Article Online
View Journal

Cite this: DOI: 10.1039/c7ob03013d

PLP-independent racemization: mechanistic and mutational studies of *O*-ureidoserine racemase (DcsC)†

Yeong-Chan Ahn, Conrad Fischer, Marco J. van Belkum and John C. Vederas *

Received 5th December 2017,
Accepted 16th January 2018

DOI: 10.1039/c7ob03013d

rsc.li/obc

O-Ureidoserine racemase (DcsC) is a PLP-independent enzyme in the biosynthetic route to the antibiotic D-cycloserine. Here we present the recombinant expression and characterization of a significantly more active DcsC variant featuring an N-terminal SUMO-tag. Synthesis of enantiomeric pure inhibitors in combination with site-specific mutation of active site cysteines to serines of this enzyme offers closer insights into the mechanism of this transformation. Homology modelling with a close relative (diaminopimelate epimerase, DapF) inspired C- and N-terminal truncation of DcsC to produce a more compact yet still active enzyme variant.

Introduction

Living cells generate predominantly L-amino acids. However, bacteria make several D-amino acids for incorporation into the peptidoglycan cell wall layer.[1,2] A number of enzymes that produce D-amino acids are racemases or epimerases based on their overall mechanistic transformation.[3] Two types of D-amino acid racemases can be found in nature: pyridoxal 5′-phosphate (PLP)-dependent and PLP-independent racemases.[4,5]

PLP-dependent racemases employ the pyridoxal cofactor to make an imine of the substrate amino acid to increase the acidity of the α-proton.[6,7] Since the pK_a of the α-position of the parent zwitterionic amino acid is about 29,[8] deprotonation at that site is unfavorable. The PLP moiety acts as an electron sink to decrease the pK_a of the α-hydrogen by delocalization of negative charge throughout the extended conjugated π-system.[7] In contrast, PLP-independent racemases generally do not require any cofactor or metal.[9–11] These enzymes can induce racemization of the α-carbon by using a thiolate–thiol pair within the active site.[12] Several PLP-independent racemases have been characterized in the literature, including glutamate racemase,[13] proline racemase,[14] aspartate racemase,[15] and isoleucine racemase.[16] One intensively studied example is diaminopimelate epimerase (DapF). DapF catalyzes the interconversion of LL-diaminopimelic acid and *meso*-diaminopimelic acid, both of which are intermediates in the biosynthesis of L-lysine in bacteria and plants.[17] Recent crystal structures of DapF reveal how this enzyme catalyzes the epimerization of substrate involving a thiol–thiolate pair[18,19] or a redox-active disulfide bridge[20,21] within the active site. In DapF, initially the active site cysteines are located near termini of α-helices in the enzyme whose dipoles reduce the thiol pK_a to generate a thiol–thiolate pair in the active site at neutral pH. Closure of the enzyme upon substrate binding expels water from the active site and generates a hydrophobic interior that enhances basicity of the thiolate. The cysteine thiolate then acts as base to deprotonate the α-carbon of the rigidly held substrate[22] and the other cysteine functions as an acid to re-protonate this site from the opposite side. DapF also decreases the pK_a of the α-proton by stereoelectronic alignment of the bond between the α-carbon and its hydrogen with the carboxylate π system.[22] In addition, extensive hydrogen bonding of the carboxylate of the substrate with amide hydrogens of the enzyme in the active site helps to increase the acidity of the α-proton.[18,23] This type of process can not be accomplished without enzymatic machinery at present.

O-Ureidoserine racemase (DcsC) is the enzyme that converts (*S*)-L-ureidoserine to (*R*)-D-ureidoserine for D-cycloserine biosynthesis in various *Streptomyces* species. It has been recently identified as PLP-independent enzyme that acts similarly to DapF (71% identity, accession number WP_078593587).[24,25] Our recent work suggested that, like DapF, DcsC also has a thiol–thiolate pair in the active site of the enzyme (Fig. 1).[25] Exploring this relationship, we decided to test the inhibition of DcsC and active site DcsC mutants with optically pure

Department of Chemistry, University of Alberta, Edmonton, AB, Canada, T6G 2G2. E-mail: john.vederas@ualberta.ca; Fax: +1-780 492 2134; Tel: +1-780 492 5475

†Electronic supplementary information (ESI) available: Compound characterization (MS sequencing, ^{1}H-NMR substrate and inhibition assays), X-ray crystal structure and analytical data (^{1}H-NMR, ^{13}C-NMR, IR, HRMS). CCDC 1588579 and 1588578. For ESI and crystallographic data in CIF or other electronic format see DOI: 10.1039/c7ob03013d

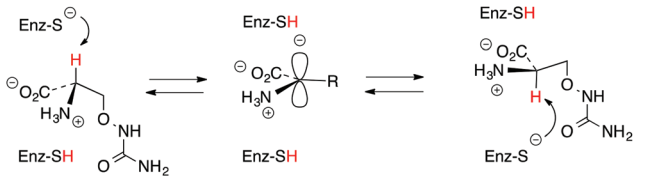

Fig. 1 Proposed epimerization of *O*-ureidoserine (**1**) catalyzed by DcsC.

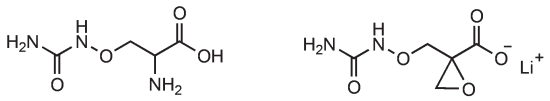

1a (*S*) L-*O*-ureidoserine
1b (*R*) D-*O*-ureidoserine

2

Scheme 1 Substrate enantiomers **1a** and **1b** and racemic inhibitor **2**.

inhibitors to obtain new insights into the enzyme's unusual mechanism. Within this paper we describe the preparation and activity of site specific mutants of DcsC as well as the synthesis of optically pure inhibitors and enzyme interaction with these inhibitors. Furthermore, the activity and kinetic performance of a truncated version of DcsC (tDcsC) are studied, presenting a more compact enzyme version. Such structural investigations would assist understanding of the distal binding site necessary for substrate side chain recognition and very strict enzyme specificity.[25]

Results and discussion

Enzyme purification and mutation of DcsC

DcsC fused to a His-tagged small ubiquitin-like modifier (SUMO) was overexpressed in *Escherichia coli* BL21(DE3). The SUMO-fusion protein was chosen to increase protein overexpression and stability, and achieve a His-tagged free DcsC protein after cleavage of the fusion tag.[26] After purification by Ni^{2+}-affinity chromatography the SUMO tag was removed by treatment with SUMO protease. The mass of the DcsC was detected by ESI-TOF (30.383 kDa, Fig. S1†). However, removal of the SUMO-tag resulted in an unstable protein that quickly precipitated even at 0 °C. Since the SUMO-tag has been shown to be beneficial for the crystallization of proteins,[27–29] we studied further properties including the tag (SUMO-DcsC, *m*/*z* 43.649 kDa, Fig. S2†).

A previous study by our group suggested locations of the active site cysteine residues responsible for the activity of a C-terminal His-tagged DcsC (Fig. 1).[25] Single-site mutation of these cysteines to serines should allow confirmation of the suggested bilateral epimerization mechanism. Therefore, site-directed mutagenesis was used to independently change Cys81 to Ser81 and Cys227 to Ser227 of SUMO-DcsC (M1-DcsC and M2-DcsC, respectively), and both enzyme mutants were isolated as described above. The loss of 16 *m*/*z* units in the respective ESI-TOF-MS (*m*/*z* 43.633 kDa, Fig. S2†) and trypsin-based MS–MS sequencing confirms the desired mutation of the M1-and M2-DcsC proteins (Fig. S3†).

To confirm the activity of the enzymes, the natural substrate isomers, L-*O*-ureidoserine (**1a**) and D-*O*-ureidoserine (**1b**) were synthesized (Scheme 1).[25] The activity of SUMO-DcsC, M1-DcsC and M2-DcsC were determined by NMR (20 mM Tris, D_2O, pD 7.6). Non-mutated SUMO-DcsC successfully exchanges the α-hydrogen of **1a** or **1b** to deuterium, as observed by disappearance of the α-H peak at 4.05 ppm after about 20 min (Fig. S4†). However, neither of the Cys → Ser mutants (M1-DcsC or M2-DcsC) showed any deuterium incorporation with either **1a** or **1b** after 24 hours. According to the proposed mechanism of DcsC, in the native enzyme both active site thiols/thiolates have important roles in deprotonation and re-protonation of the α-position of **1**. Hence, in both enzyme mutants, deprotonation of the α-carbon of the substrate by the single active site thiolate, if it occurs at all, does not result in exchange with solvent. The racemization process does not occur, presumably because of the significantly higher pK_a of an active site serine as a proton donor on the opposite side.

Inhibition of SUMO-DcsC and mutants

To show that the active site of DcsC consists of a thiol–thiolate pair, the irreversibly-binding oxirane inhibitor **2** was synthesized in racemic form (Scheme 1).[25] Similar to the aziridine-based inhibition of glutamate racemase[30] and diaminopimelate epimerase,[23,31–34] it was expected that the epoxide ring would react with an active site cysteine, giving rise to a covalent attachment (Fig. 2). Each cysteine in the active site is expected to be inhibited by one enantiomer of the inhibitor at a time (Fig. 2) resulting in an *m*/*z*-peak of increased mass (43.825 kDa for SUMO-DcsC). The enzyme mutants (M1-DcsC, M2-DcsC) each were also successfully inhibited by racemic inhibitor **2**, indicated by additional mass peaks in the

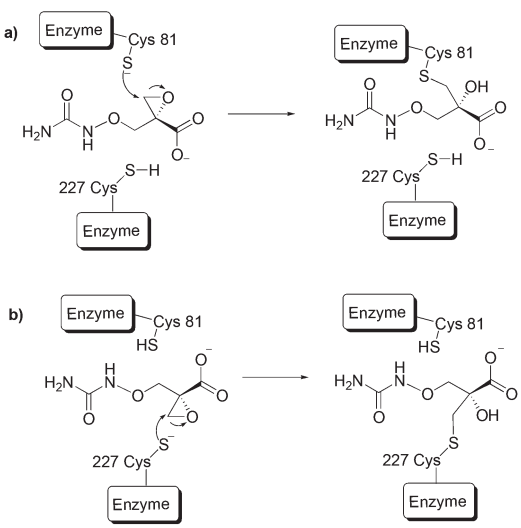

Fig. 2 a. Putative inhibition of Cys81 by (*S*)-Inhibitor. b. Putative inhibition of Cys227 by (*R*)-Inhibitor.

ESI-TOF-MS spectra (Fig. S2†). The difference between two main peaks in the mass spectra is 176 Da (*m*/*z* ratio), corresponding to the molecular weight of **2**. MS–MS sequencing data confirmed the desired sites of inhibition (Fig. S3†). These results suggest that SUMO-DcsC and the mutants can be inhibited by racemic oxirane inhibitor **2**. However, SUMO-DcsC and both mutants showed low inhibition (less than 40%, Fig. S2†), and we were not able to obtain crystals from these proteins to solve the protein structure.

Synthesis of chiral inhibitors

To investigate the mechanism of DcsC (Fig. 2), we targeted the synthesis of the optically pure inhibitors **2a** and **2b**. Since racemic oxirane inhibitor **2** was somewhat unstable under aqueous conditions at room temperature due to epoxide ring opening, we chose to synthesize stable diastereomeric ester precursor mixtures **7a**/**8a** and **7b**/**8b** and to separate pure enantiomers from them (Scheme 2). Hydrolysis of each stereochemically pure ester would then give the optically pure inhibitors. (*S*)-1-Phenylethanol (**4a**) and (*R*)-1-phenylethanol (**4b**) were used as chiral entries for the synthesis. Briefly, bromoacrylic acid was esterified separately with either alcohol **4a** or **4b** in a Mitsunobu reaction. The bromoesters (**5a** and **5b**) were treated individually with *tert*-butyl peroxide, using NaH as base in ether. Peroxides **6a** and **6b** were then reacted with hydroxyurea to form the diastereomeric precursor inhibitor mixtures **7a**/**8a** and **7b**/**8b**, respectively. The diastereomeric inhibitors in each mixture were separated by recrystallization. Repeated recrystallization from a benzene–EtOAc mixture (2 : 1) gave enantiomerically pure precursors **7a** and **7b**, whose structures were confirmed by X-ray diffraction analysis (Fig. S5, Table S1†). Saponification of each by LiOH furnishes the pure chiral inhibitors **2a** and **2b**, respectively. Both inhibitors (10 eq.) were separately added to M1-DcsC and M2-DcsC mutants and samples were submitted to ESI-TOF-MS analysis to identify and confirm the sites of inhibition. Whereas M1-DcsC was only inhibited by **2a**, the M2-DcsC mutant was inhibited by **2b** (Fig. 3 and Fig. S6†).

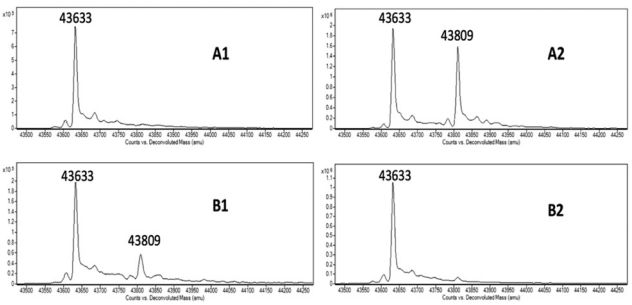

Fig. 3 Electrospray mass spectra of inhibited M1-DcsC mutants (A1: **2a**, A2: **2b**) and M2-DcsC mutants (B1: **2a**, B2: **2b**). The nominal mass of the inhibitor is 176 Da.

In addition, MS–MS sequencing data confirmed the inhibition sites (Fig. S7†). These data indicate that the free active site cysteine in both mutants (C227 in M1-DcsC and C81 in M2-DcsC) can each only react with one inhibitor enantiomer, thus supporting the bilateral reaction mechanism (Fig. 2).

Truncation of DcsC

To obtain additional structural information about DcsC, we compared the modeled structure of the protein to the reported coordinates of DapF from *Haemophilus influenzae* (PDB: 1bwz, Fig. 4).[18] Closer examination reveals a flexible N- and C-terminus of DcsC consisting of 9 and 3 amino acids, respectively (Fig. S8†). Truncation of these less-structured segments could result in an enzyme (tDcsC) that maintains catalytic activity, but has improved stability. In contrast to the SUMO-DcsC, we were not able to cleave the SUMO-tag from tDcsC after purification. Hence for activity testing, SUMO-

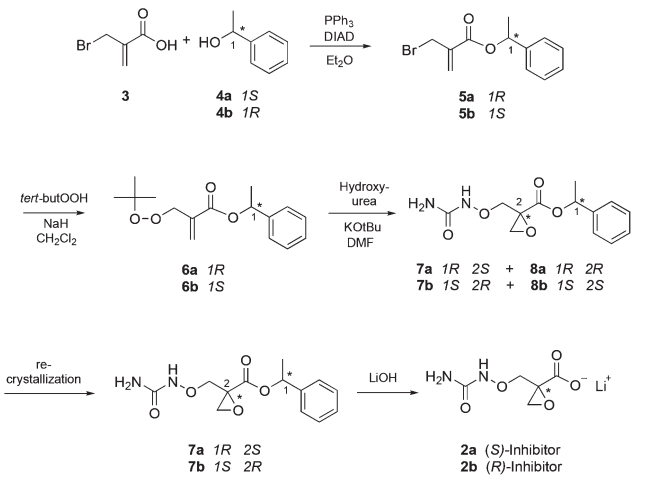

Scheme 2 Synthesis of chiral oxirane inhibitors.

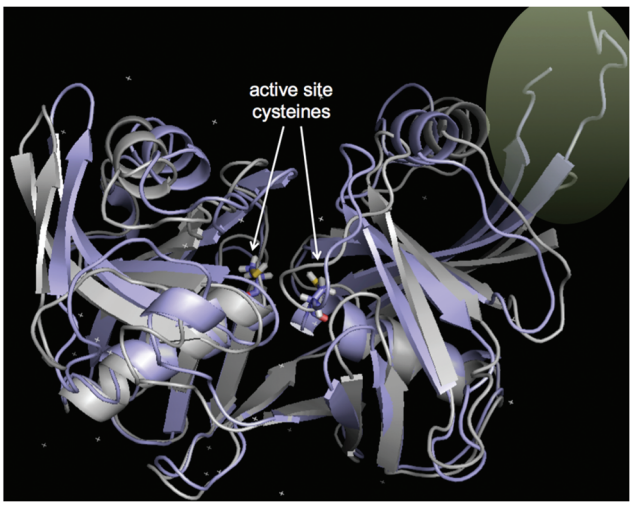

Fig. 4 Ribbon-model structure of DcsC (lightblue) based on the modeling of DapF from *Haemophilus influenzae* (gray, PDB ID: 1bwz, Seq. identity: 42%). The truncated areas (C- and N-terminal) are highlighted in green.

Table 1 Kinetic parameters of DcsC variants

Species	Direction	v_{max} (mM s^{-1})	K_m (mM)	K_{cat} (1 s^{-1})	K_{cat}/K_m (1 M^{-1} s^{-1})	Ref.
DcsC-His_6	**1a** → **1b**	0.084	110	158	1436	25
DcsC-His_6	**1b** → **1a**	0.015	17	29	1706	25
SUMO-DcsC	**1a** → **1b**	0.022	12	475	41 130	—
SUMO-DcsC	**1b** → **1a**	0.047	32	1450	45 302	—
DcsC (tag-free)	**1a** → **1b**	<0.001	n.d.	n.d.	n.d.	—
DcsC (tag-free)	**1b** → **1a**	<0.001	n.d.	n.d.	n.d.	—
SUMO-tDcsC	**1a** → **1b**	0.042	15	315	21 137	—
SUMO-tDcsC	**1b** → **1a**	0.046	22	194	8642	—

tDcsC was incubated with the natural substrates **1a** and **1b** (20 mM Tris, D_2O, pD 7.6). The activity profiles of SUMO-tDcsC are somewhat lower compared to the native enzyme (see below).

In order to characterize the inhibition properties of SUMO-tDcsC, mutants M1-tDcsC and M2-tDcsC were generated that incorporate a serine for cysteine mutations in the active site in analogous fashion to those generated in the native protein (Cys72 → Ser in M1-tDcsC and Cys218 → Ser in M2-tDcsC). ESI-TOF-mass spectra reveal the proteins of desired mass (tDcsC: 42 317 Da, M1-tDcsC and M2-tDcsC: 42 301 Da, Fig. S9†). The sequence was confirmed to be correct by applying MS–MS digest analysis (Fig. S10†). Incubation of both mutants with the natural substrates **1a** and **1b** as before showed no activity, underlining the proposed bilateral mechanism. Both mutants were almost completely inhibited by the expected compatible enantiomer **2a** or **2b** (Fig. S9†). However, a second site of alkylation becomes available in the truncated versions (Cys41), indicated by a small additional mass peak (Fig. S9†). This suggests a somewhat looser structure with greater access for inhibitors to the enzyme interior.

Kinetic parameters of various DcsC variants

The catalytic parameters for various DcsC variants were determined by time-dependent ^{1}H-NMR spectroscopy and are summarized in Table 1. The catalytic parameters for the C-terminal His-tagged enzyme version of DcsC published previously[25] are also included in this table for reference. The data were extracted from the signal ratio between the vanishing α-hydrogen (at δ ~4.05 ppm) and the β-hydrogen (at δ ~4.2 ppm) (Fig. S11†). The initial velocities (3 min) were used to calculate the Michaelis–Menten parameters. In general, these calculations reveal two trends: the catalytic efficiency (K_{cat}/K_m) in both directions is almost 30-times higher for the SUMO-tagged DcsC version in comparison to the His-tagged enzyme version. One possible explanation for this enhanced catalytic performance could be the predominantly dimeric state of SUMO-DcsC compared to a higher oligomeric state of the His-tagged version (compare Fig. S12†), which has been described as catalytic accelerator for other racemases.[35] Truncation of the enzyme (SUMO-tDcsC, Table 1) renders these variants 50–80% less active than the native version but still 5–14-times more active than the C-terminally His-tagged variant. Removal of the SUMO-tag results in an instable protein that quickly precipitates even at 0 °C, preventing determination of kinetic parameters. Unlike for the His-tagged DcsC version, the substrate affinity towards the *O*-ureidoserine enantiomers (direction of transformation, **1a** → **1b** or **1b** → **1a**) is comparable for the SUMO-tagged variants.

Conclusions

Herein we report the recombinant expression of *O*-ureidoserine racemase (DcsC) featuring an N-terminal SUMO-tag. Purified SUMO-DcsC racemizes the natural substrates L- and D-*O*-ureidoserine **1a** and **1b** with a 30-fold increased catalytic activity in comparison to a C-terminally His-tagged enzyme version. Individual mutation of both active site cysteines and incubation with inhibitor enantiomers **2a** and **2b** reveals selective inactivation depending on the chirality of the inhibitor, thus supporting the bilateral reaction mechanism of the enzyme. Truncation of the C- and N-terminal ends of the protein as well as removal of the SUMO-tag results in a de-stabilization of the protein structure and reduction of the enzyme activity. Crystallization studies are underway ultimately aiming to obtain a single X-ray structure of the enzyme, which will help us to rationalize the interior dimensions and distal site recognition of the active site.

Experimental

Fusion protein expression and purification

DNA sequences encoding DcsC and tDcsC were purchased from BioBasic Inc. (Ontario, Canada) and cloned separately into the pET SUMO (small ubiquitin-like modifier) expression vector (Invitrogen). Clones were sequenced to confirm that DcsC and tDcsC were in frame with the His-tagged SUMO fusion protein. The resulting pET SUMO-DcsC and pET SUMO-tDcsC plasmids were transformed into *Escherichia coli* BL21 (DE3). For protein expression, the *E. coli* transformant was grown in 1 L LB Broth, Miller (Luria–Bertani) (10 g of tryptone, 5 g of yeast extract, 10 g of NaCl) at 37 °C with shaking (225 rpm) to an optical density (OD_{600}) of 0.6–0.8 using kanamycin as selective pressure. Next, the cells were chilled in an ice bath for 10 minutes before IPTG (0.2 mM) was added to the culture to induce protein expression. The culture was then incubated at 23 °C for 16 hours with shaking (225 rpm). The cells were

harvested by centrifugation (6300 rpm, 4 °C, 30 min) and suspended in lysis buffer [100 mM sodium-phosphate (pH 7.8), 300 mM NaCl, 20 mM imidazole, 1 mM EDTA] with 2 mg of lysozyme and 10 unit of DNase I (Thermo Scientific). The cells were lysed using a Constant Systems Cell Disruptor, model TS (Constant Systems, Ltd) operated at 20 kpsi. The lysate was centrifuged (15 000 rpm, 30 min), and the supernatant containing the fusion protein was isolated. The lysate was mixed with Ni-NTA resin (Qiagen), and loaded on a fritted column. The resin was washed with 20 mL lysis buffer, and the fusion protein was eluted with 10 mL lysis buffer containing 300 mM imidazole. The fusion protein solution was dialyzed against 3 L of buffer [20 mM Tris-HCl (pH 7.8), 5 mM DTT] for 20 h at 4 °C and concentrated by centrifugation using an Amicon Ultra centrifugal filter (30 kDa, 4000*g*, 20 min). Average recovery was 10–30 mg L^{-1} culture.

Cleavage of fusion protein

To cleave the SUMO tag, approximately 20 mg of fusion protein was incubated with 25 units of His-tagged SUMO protease (McLab, South San Francisco, CA) in 50 mM Tris-HCl (pH 8.0), 1 mM DTT, 0.2% Igepal CA-360 (Sigma) and 150 mM NaCl in a total volume of 5 mL. Digestion of the fusion protein was performed for 20 h at 4 °C. Cleavage of the fusion protein checked by sodium dodecyl sulfate-polyacrylamide gel electrophoresis (SDS-PAGE). The cleavage mixture was added to 1 mL of Ni-NTA agarose (Qiagen) resin and loaded on a fritted column to remove the His-tagged SUMO and His-tagged SUMO protease. The flow through containing the enzyme was collected and checked for purity by SDS-PAGE. The enzyme solution was then dialyzed against 3 L of buffer [20 mM Tris-HCl (pH 7.8), 5 mM DTT] for 20 h at 4 °C and concentrated by centrifugation using an Amicon Ultra centrifugal filter (30 kDa, 4000*g*, 20 min). Average yield was around 7 mg of enzyme.

Site-directed mutagenesis of DcsC and tDcsC enzymes

QuikChange II Site-Directed Mutagenesis Kit (Agilent Technologies) was used to construct plasmids encoding DcsC and tDcsC with cysteine to serine residues mutations in the active site according to the manufacturer's instructions. Primer pair MVB206 (5′-CCGTTCCGCGCAGTCTGGCAACGG TGCACG-3′) and MVB207 (5′-CGTGCACCGTTGCCAGACTGCG CGGAACGG-3′) was used to create the C81S mutation, whereas primer pair MVB208 (5′-GTGAAACCCTGGCGTCCGGTTCC GGTGCATG-3′) and MVB209 (5′-CATGCACCGGAACCGG ACGCCAGGGTTTCAC-3′) was used to create the C227S mutation. The presence of these mutations was verified by nucleotide sequencing of the whole coding region. The resulting plasmids were transformed into *E. coli* BL21(DE3) to overexpress and isolate the mutant enzymes.

General information

All non-aqueous reactions were done with oven-dried glassware under argon. Solvents were dried by follows: CH_2Cl_2 was distilled over CaH_2; tetrahydrofuran (THF) was distilled over Na; EtO_2 was distilled over Na; MeOH, EtOH, acetonitrile as well as DMF were dried over activated 4 Å molecular sieves. ^{1}H-NMR (600 MHz/400 MHz) and ^{13}C-NMR (151 MHz/125 MHz) data were obtained on a Agilent/Varian VNMRS four-channel spectrometer at room temperature with TMS or the solvent signal as internal standard. High-resolution mass spectra were recorded on an Agilent 6220 oaTOF with electron ionization. IR-spectra were measured using a Nicolet 8700 spectrometer. Specific rotation was measured on a Sodium D line (589 nm) with PerkinElmer 241 Polarimeter. Circular dichroism spectra were recorded on an OLIS globalworks CD spectrophotometer. Staring compound **3** and (*R*)-1-phenylethanol, (*S*)-1-phenylethanol are commercially available from Sigma-Aldrich.

1-Phenylethyl-2-bromomethyl acrylate [5a, 5b]

To a solution of bromomethylacrylic acid **3** (1.50 g, 9.09 mmol) and diisopropyl azodicarboxylate (DIAD) (1.80 mL, 9.14 mmol) in diethyl ether (15 mL), was added a solution of (*S*)-1-phenylethanol **4a** (1.20 mL, 9.90 mmol) and triphenylphosphine (2.36 g, 9.09 mmol) in diethyl ether (15 mL), dropwise at 0 °C. The mixture was stirred at the same temperature for 30 min, and then at room temperature for 48 h. The mixture was filtered and washed with Et_2O (20 mL). After concentration of the filtrate, the crude product was purified by flash column chromatography (5% EtOAc in hexanes) to furnish the acrylate as a yellow liquid (1.47 g, 60%).

5a (*R*). ^{1}H-NMR (600 MHz, $CDCl_3$) δ 7.40 (m, 5H, Ph–**H**), 6.39 (d, 1H, J = 1.0 Hz, =C**H**), 6.01 (d, 1H, J = 1.0 Hz, =C**H**), 5.95 (q, 1H, J = 6.9 Hz, Ph–C**H**), 4.21 (dd, 2H, J = 2.5, 1.0 MHz, Br–C**H**$_2$), 1.58 (d, 3H, J = 8.5 Hz, CH–C**H**$_3$). ^{13}C-NMR (150 MHz, $CDCl_3$) δ 20.3, 21.2, 28.5, 73.4, 125.6, 127.5, 128.1, 128.3, 138.3, 141.5, 164.1. $[\alpha]_D^{25}$ = +23.24 (c = 0.500, CH_2Cl_2). IR (thin film) ν 3087, 3063, 2960, 2930, 2872, 1722, 1632, 1453, 1186 cm^{-1}. HRMS (ESI) $[M + Na]^+$ m/z calcd for $C_{12}H_{13}BrNaO_2$: 290.9991, found 290.9991.

5b (*S*). Starting with (*R*)-1-phenylethanol **4b**. ^{1}H-NMR (600 MHz, $CDCl_3$) δ 7.40 (m, 5H, Ph–**H**), 6.39 (d, 1H, J = 1.0 Hz, =C**H**), 6.01 (d, 1H, J = 1.0 Hz, =C**H**), 5.95 (q, 1H, J = 6.9 Hz, Ph–C**H**), 4.25 (dd, 2H, J = 2.5, 1.0 MHz, Br–C**H**$_2$), 1.58 (d, 3H, J = 6.4 Hz, CH–C**H**$_3$). ^{13}C-NMR (150 MHz, $CDCl_3$) δ 20.1, 21.3, 28.4, 73.5, 125.7, 127.5, 128.0, 128.3, 138.1, 141.5, 164.1. $[\alpha]_D^{25}$ = −26.71 (c = 0.500, CH_2Cl_2). IR (thin film) ν 3087, 3064, 2980, 2931, 2872, 1722, 1632, 1453, 1187 cm^{-1}. HRMS (ESI) $[M + Na]^+$ m/z calcd for $C_{12}H_{13}BrNaO_2$: 290.9991, found 290.9991.

1-Phenylethyl-2-*tert*-butylperoxomethyl acrylate [6a, 6b]

A solution of *tert*-butylhydroperoxide (1.50 mL, 8.26 mmol) in dry CH_2Cl_2 (20 mL) was stirred at −5 °C under a stream of argon. To this was added sodium hydride (0.28 g, 7.0 mmol, 60% dispersion in mineral oil). After 15 minutes, **5a** or **5b** (1.47 g, 5.48 mmol) was added by dropwise at −5 °C. After 4 h, the mixture was filtered and washed with dry CH_2Cl_2. After concentration of the filtrate, the crude product was purified by flash column chromatography (4% EtOAc in hexanes) to obtain **6a** or **6b** as a yellow liquid (0.72 g, 46%).

6a (*R*). ^{1}H-NMR (600 MHz, $CDCl_3$) δ 7.38 (m, 5H, Ph–**H**), 6.35 (d, 1H, J = 1.0 Hz, =C**H**), 5.91 (d, 1H, J = 1.0 Hz, =C**H**), 5.94 (q, 1H, J = 6.6 Hz, Ph–C**H**), 4.63 (dd, 2H, J = 3.0, 1.0 MHz, O–C**H**$_2$), 1.58 (d, 3H, J = 7.0 Hz, CH–C**H**$_3$), 1.18 (s, 9H, O–C–C**H**$_3$); ^{13}C-NMR (150 MHz, $CDCl_3$) δ 21.1, 25.1, 72.7, 79.8, 125.8, 127.5, 128.2, 136.7, 141.8, 165.0. $[\alpha]_D^{25}$ = +20.73 (c = 0.500, CH_2Cl_2). IR (thin film) ν 3089, 3065, 3034, 2980, 2932, 2874, 1723, 1637, 1454, 1363, 1162 cm^{-1}. HRMS (ESI) $[M + Na]^+$ m/z calcd for $C_{16}H_{22}NaO_4$ 301.1410, found 301.1409.

6b (*S*). ^{1}H-NMR (600 MHz, $CDCl_3$) δ 7.38 (m, 5H, Ph–**H**), 6.35 (d, 1H, J = 1.0 Hz, =C**H**), 5.91 (d, 1H, J = 1.0 Hz, =C**H**), 5.94 (q, 1H, J = 6.6 Hz, Ph–C**H**), 4.63 (dd, 2H, J = 3.0, 1.0 MHz, O–C**H**$_2$), 1.58 (d, 3H, J = 7.0 Hz, CH–C**H**$_3$), 1.18 (s, 9H, O–C–C**H**$_3$); ^{13}C-NMR (150 MHz, $CDCl_3$) δ 21.4, 25.2, 72.9, 79.9, 125.6, 127.5, 128.1, 136.6, 141.7, 165.1. $[\alpha]_D^{25}$ = −19.23 (c = 0.500, CH_2Cl_2). IR (thin film) ν 3088, 3065, 3034, 2980, 2932, 2873, 1724, 1638, 1454, 1363, 1162 cm^{-1}. HRMS (ESI) $[M + Na]^+$ m/z calcd for $C_{16}H_{22}NaO_4$ 301.1410, found 301.1410.

(*R*)-1-Carboxy-(1-phenylethyl)-1-*O*-ureido-methoxy oxiranes 7a (1*R*,2*S*) and 8a (1*R*,2*R*)

Compound **6a** (*R*) (0.720 g, 2.58 mmol) and hydroxyurea (0.250 g, 3.28 mmol) were dissolved in dry DMF (15 mL), and the mixture was cooled to 0 °C on an ice-water bath. To this mixture was added a potassium *tert*-butoxide solution (0.80 mL, 0.80 mmol, 1 M in THF) dropwise, and the solution turned light yellow. The mixture was stirred at 0 °C for 30 min, and another 4 h at room temperature. Solvent was then removed by a rotary evaporator attached to high-vacuum. The crude yellow mixture was applied to silica gel chromatography (9 : 1 EtOAc : hexane, then pure EtOAc), to yield the diastereomers **7a** (1*R*,2*S*) and **8a** (1*R*,2*R*) as a yellowish solid–liquid mixture (0.17 g, 23%). Repeated re-crystallization from benzene/EtOAc yielded **7a** (1*R*,2*S*) as crystalline material.

^{1}H-NMR (600 MHz, $CDCl_3$) δ 7.38 (m, 5H, Ph–**H**), 5.94 (q, 1H, J = 6.5 Hz, Ph–C**H**), 4.41(d, 1H, J = 10.1 Hz, C**H**$_2$ONH), 4.13 (d, 1H, J = 10.1 Hz, C**H**$_2$ONH), 3.16 (d, 1H, J = 6.0 Hz, oxirane-C**H**$_2$), 3.02 (d, 1H, J = 6.0 Hz), 1.61 (d, 3H, J = 6.5 Hz, CH–C**H**$_3$); ^{13}C-NMR (150 MHz, $CDCl_3$) δ 21.8, 50.1, 74.2, 75.1, 124.8, 128.2, 128.8, 165.4 IR (thin film) ν 3415, 3392, 3174, 3040, 2989, 2940, 2878, 1718, 1682, 1457, 1373, 1176 cm^{-1}. HRMS (ESI) $[M + Na]^+$ m/z calcd for $C_{13}H_{16}N_2O_5Na$ 303.0951, found 303.0954.

Evaporation of the filtrate after re-crystallization gave pure **8a** (1*R*,2*R*). ^{1}H-NMR (600 MHz, $CDCl_3$) δ 7.38 (m, 5H, Ph–**H**), 5.94 (q, 1H, J = 6.5 Hz, Ph–C**H**), 4.37 (d, 1H, J = 10.1 Hz, C**H**$_2$ONH), 4.05 (d, 1H, J = 10.1 Hz, C**H**$_2$ONH), 3.23 (d, 1H, J = 6.0 Hz, oxirane-C**H**$_2$), 2.96 (d, 0.6H, J = 6.0 Hz), 1.61 (d, 3H, J = 6.5 Hz, CH–C**H**$_3$); ^{13}C-NMR (150 MHz, $CDCl_3$) δ 21.8, 50.1, 74.2, 75.1, 124.8, 128.2, 128.8, 165.2. HRMS (ESI) $[M + Na]^+$ m/z calcd $C_{13}H_{16}N_2O_5Na$ 303.0951, found 303.0952.

(*S*)-1-Carboxy-(1-phenylethyl)-1-*O*-ureido-methoxy oxiranes 7b (1*S*,2*R*) and 8b (1*S*,2*S*)

Compound **6b (*S*)** (0.72 g, 2.58 mmol) and hydroxyurea (0.25 g, 3.28 mmol) were dissolved in dry DMF (15 mL), and the mixture was cooled to 0 °C on an ice-water bath. To this mixture was added a potassium *tert*-butoxide solution (0.80 mL, 0.80 mmol, 1 M in THF) dropwise, and the solution turned light yellow. The mixture was stirred at 0 °C for 30 min, and another 4 h at room temperature. Solvent was then removed by a rotary evaporator attached to high-vacuum. The crude yellow mixture was applied to silica gel chromatography (9 : 1 EtOAc : hexane, then pure EtOAc), to yield the diastereomers **7b** (1*S*,2*R*) and **8b** (1*S*,2*S*) as a yellowish solid–liquid mixture (0.17 g, 23%). Repeated re-crystallization from benzene/EtOAc yielded **7b** (1*S*,2*R*) as crystalline material.

^{1}H-NMR (600 MHz, $CDCl_3$) δ 7.38 (m, 5H, Ph–**H**), 5.94 (q, 1H, J = 6.5 Hz, Ph–C**H**), 4.41(d, 1H, J = 10.1 Hz, C**H**$_2$ONH), 4.13 (d, 1H, J = 10.1 Hz, C**H**$_2$ONH), 3.16 (d, 1H, J = 6.0 Hz, oxirane-C**H**$_2$), 3.02 (d, 1H, J = 6.0 Hz), 1.61 (d, 3H, J = 6.5 Hz, CH–C**H**$_3$); ^{13}C-NMR (150 MHz, $CDCl_3$) δ 21.6, 50.3, 74.7, 124.8, 128.2, 128.8, 165.3. IR (thin film) ν 3415, 3392, 3171, 3041, 2989, 2939, 2877, 1719, 1683, 1457, 1373, 1177 cm^{-1}. HRMS (ESI) $[M + Na]^+$ m/z calcd for $C_{13}H_{16}N_2O_5Na$ 303.0951, found 303.0950. Evaporation of the filtrate and re-crystallization gave pure **8b (1*S*,2*S*)** showing identical analytical data as the 1*R*,2*R*-compound obtained from the (*R*)-precursor.

1-Carboxy-1-*O*-ureido-methoxy-(*S*)-oxirane 2a (*S*)

Ester **7a** (1*R*,2*S*) (1.0 mg, 0.004 mmol) was saponified in D_2O (0.7 mL) containing LiOH solution (0.010 mL, 0.010 mmol, 1 M solution in D_2O). After 10 min, the reaction was deemed to be complete by ^{1}H-NMR, and the solvent was removed by lyophilization.

^{1}H-NMR (600 MHz, $CDCl_3$) δ (600 MHz, D_2O) 4.43 (d, 1H, J = 10.2 Hz, C**H**$_2$ONH), 3.72 (d, 1H, J = 10.1 Hz, C**H**$_2$ONH), 2.95 (s, 2H, oxirane-C**H**$_2$); ^{13}C-NMR (150 MHz, $CDCl_3$) δ 49.2, 57.1, 78.5, 163.1, 174.5 IR (thin film) ν 3301 (broad), 2938, 1671, 1619, 1425, 1107 cm^{-1}. HRMS (ESI) $[M - H]^-$ m/z calcd for $C_5H_7N_2O_5$ 175.0360, found 175.0357.

1-Carboxy-1-*O*-ureido-methoxy-(*R*)-oxirane 2b (*R*)

Ester **7b** (1*S*,2*R*) (1.0 mg, 0.04 mmol) was saponified in D_2O (0.7 mL) containing LiOH solution (0.010 mL, 0.010 mmol, 1 M solution in D_2O). After 10 min, the reaction was deemed to be complete by ^{1}H-NMR, and the solvent was removed by lyophilization.

^{1}H-NMR (600 MHz, $CDCl_3$) δ (600 MHz, D_2O) 4.43 (d, 1H, J = 10.2 Hz, C**H**$_2$ONH), 3.72 (d, 1H, J = 10.1 Hz, C**H**$_2$ONH), 2.95 (s, 2H, oxirane-C**H**$_2$); ^{13}C-NMR (150 MHz, $CDCl_3$) δ 49.2, 57.2, 78.5, 163.3, 174.7 IR (thin film) ν 3301 (broad), 2938, 1671, 1619, 1425, 1107 cm^{-1}. HRMS (ESI) $[M - H]^-$ m/z calcd for $C_5H_7N_2O_5$ 175.0360, found 175.0358.

General protocol for methanolysis of cycloserine[25]

The literature procedure was adapted.[25] Acetyl chloride (7.14 mL, 100 mmol) was added to dry methanol (100 mL) cooled in an ice bath and stirred under argon for 15 min. Next, 1.00 g of enantiomerically pure cycloserine (9.80 mmol) was dissolved in the acidic methanol solution and warmed to room temperature. After 15 min, a reflux condenser was connected

to flask, and the mixture was stirred for 15 h at 70 °C. Insoluble materials were removed by filtration, and solvent was removed by a rotary evaporator. Ethyl acetate (700 mL) was added to recrystallize the product, and white solid was precipitated after an hour of stirring. The *O*-aminoserine methyl ester (1.25 g) was filtered and analyzed by NMR and CD, which displayed expected properties.[25]

General ureidoylation and saponification protocol

The literature procedure was adapted.[25] *O*-Aminoserine methyl ester (300 mg, 2.20 mmol) was dissolved in 10 mL water, and potassium cyanate (180 mg, 2.22 mmol) was added to the solution. pH of solution was adjusted to 4–5 to get maximal yield, and the solution was stirred for 2 h at room temperature. When the reaction was finished as determined by TLC, the solution was adjusted to pH ~1 with 1 M HCl to terminate the reaction. Solvent was removed by rotatory evaporator, and the oily ester product was used for next reaction without purification. The ester was dissolved in 20 mL of water and 2 M potassium hydroxide (2 ml, 4.0 mmol) was added. The mixture was stirred at room temperature until the reaction was finished as determined by TLC (NH_4OH : i-PrOH = 3 : 7). The mixture was adjusted to pH 4 with 1 M HCl to terminate the reaction, and excess EtOH (20 mL) was added to precipitate the product. Solvent was evaporated by rotatory evaporator, and the product was purified by Varian BondElut C18 SPE cartridge. The cartridge was washed with water first (20 mL), and a water solution of crude compound was loaded to cartridge. The product was eluted with water (10 mL) and then MeCN–H_2O (1 : 1) solution. The fractions containing product were collected and lyophilized to yield the pure isomer of *O*-ureidoserine **1** as a solid.

X-ray diffraction

Crystals of **7a** (1*R*,2*S*) and **7b** (1*S*,2*R*), suitable for analysis were obtained by slow cooling of a hot solution of each pure isomer in benzene/EtOAc (2 : 1). The intensity data were collected on a Bruker APEX II diffractometer with CuKα radiation (λ = 1.5418 Å) using ω- and φ-scans. Reflections were corrected for background and Lorentz polarization effects. Preliminary structure models were derived by application of direct methods and were refined by fullmatrix least squares calculation based on F^2 for all reflections. All hydrogen atoms were included in the models in calculated positions and were refined as constrained to bonding atoms. The crystal data and experimental parameters are summarized in the ESI and the structures are deposited under CCDC 1588579 (**7a**) and CCDC 1588578 (**7b**).†

Enzyme kinetics monitoring by ^{1}H-NMR

To analyze the kinetics of truncated DcsC by NMR, enantiomerically pure ureidoserine (2–15 mM) was dissolved to Tris buffer (D_2O, 20 mM, pD = 7.8). To initiate the reaction, truncated DcsC (3–6 μg) was added and ^{1}H NMR was recorded every 3 min. To determine enzyme activity, the peak of β-CH_2 peak (mutiplet, 4.2–4.3 ppm) was compared with the α-CH peak (triplet, 3.9–4.0 ppm). Since truncated DcsC exchanges the α-CH to α-CD, the progress of the reaction was monitored by the disappearance of the α-CH peak.

Enzyme kinetics monitoring by CD spectroscopy

The ureidoserine samples (300 μL, 2–15 mM, phosphate buffer (pH = 7.8), 1 mM DTT) were placed in 1 mm quartz cell, and reactions were monitored at 30 °C, at 206 nm. The CD signal (in mdeg) was recorded every two seconds, for five minutes. The reaction was initiated by adding truncated DcsC (2–5 μg), and the quartz cell was directly placed in CD spectrophotometer. The data were processed to Excel and GraphPad prism. The enzyme initial velocity (V_o) was calculated within the linear range of the CD-signal decay (initial 2 minutes), and kinetics were extracted using Michaelis–Menten analysis.

Conflicts of interest

There are no conflicts to declare.

Acknowledgements

The authors gratefully acknowledge Dr Robert McDonald and Dr Michael Ferguson (University of Alberta) for X-ray crystallographic analyses, Mark Miskolzie (University of Alberta Nuclear Magnetic Resonance Laboratory) for NMR analyses, Wayne Moffat and Jennifer Jones (University of Alberta Analytical and Instrumentation Laboratory) for IR and CD analyses, Gareth Lambkin (University of Alberta) for biological services, and Jing Zheng and Bela Reiz (University of Alberta Mass Spectrometry Laboratory). This work was supported by the Natural Sciences and Engineering Research Council of Canada (NSERC) and Alberta Innovates Health Solutions (AIHS Fellowship to CF) for financial support.

Notes and references

1 R. J. Thompson, G. H. Bouwer, D. A. Portnoy and F. R. Frankel, *Infect. Immun.*, 1998, **66**, 3552–3561.
2 N. E. Caceres, N. B. Harris, J. F. Wellehan, Z. Feng, V. Kapur and R. G. Barletta, *J. Bacteriol.*, 1997, **179**, 5046–5055.
3 K. Soda and N. Esaki, *Pure Appl. Chem.*, 1994, **66**, 709–714.
4 S. Y. Choi, N. Esaki, M. Ashiuchi, T. Yoshimura and K. Soda, *Proc. Natl. Acad. Sci. U. S. A.*, 1994, **91**, 10144–10147.
5 C. T. Walsh, *J. Biol. Chem.*, 1989, **264**, 2393–2396.
6 S. Sun and M. D. Toney, *Biochemistry*, 1999, **38**, 4058–4065.
7 J. C. Vederas and H. G. Floss, *Acc. Chem. Res.*, 1980, **13**, 455–463.
8 J. P. Richard, T. L. Amyes, B. Goryanova and X. Zhai, *Curr. Opin. Chem. Biol.*, 2014, **21**, 1–10.
9 M. E. Tanner, *Acc. Chem. Res.*, 2002, **35**, 237–246.
10 A. D. Radkov and L. A. Moe, *Appl. Microbiol. Biotechnol.*, 2014, **98**, 5363–5374.

11 N. Bernardo-García, P. Sánchez-Murcia, F. Gago, F. Cava and J. A. Hermoso, *Curr. Org. Chem.*, 2016, **20**, 1222–1231.
12 P. Conti, L. Tamborini, A. Pinto, A. Blondel, P. Minoprio, A. Mozzarelli and C. De Micheli, *Chem. Rev.*, 2011, **111**, 6919–6946.
13 T. Lundqvist, S. L. Fisher, G. Kern, R. H. A. Folmer, Y. Xue, D. T. Newton, T. A. Keating, R. A. Alm and B. L. M. de Jonge, *Nature*, 2007, **447**, 817–822.
14 A. Buschiazzo, M. Goytia, F. Schaeffer, W. Degrave, W. Shepard, C. Grègoire, N. Chamond, A. Cosson, A. Berneman, N. Coatnoan, P. M. Alzari and P. Minoprio, *Proc. Natl. Acad. Sci. U. S. A.*, 2006, **103**, 1705–1710.
15 L. Liua, K. Iwatab, M. Yohdab and K. Mikia, *FEBS Lett.*, 2002, **528**, 114–118.
16 R. C. Strauch, E. Svedin, B. Dilkes, C. Chapple and X. Li, *Proc. Natl. Acad. Sci. U. S. A.*, 2015, **112**, 11726–11731.
17 C. W. Koo and J. S. Blanchard, *Biochemistry*, 1999, **38**, 4416–4422.
18 B. Pillai, M. M. Cherney, C. M. Diaper, A. Sutherland, J. S. Blanchard, J. C. Vederas and M. N. G. James, *Proc. Natl. Acad. Sci. U. S. A.*, 2006, **103**, 8668–8673.
19 L. Hor, R. C. J. Dobson, C. Dogovski, C. A. Hutton and M. A. Perugini, *Acta Crystallogr., Sect. F: Struct. Biol. Cryst. Commun.*, 2010, **66**, 37–40.
20 H.-Y. Sagong and K.-J. Kim, *Sci. Rep.*, 2017, **7**, 42318.
21 J. S. Park, W. C. Lee, J. H. Song, S. I. Kim, J. C. Lee, C. Cheong and H.-Y. Kim, *Acta Crystallogr., Sect. F: Struct. Biol. Cryst. Commun.*, 2013, **69**, 42–44.
22 M. H. Gelb, Y. Lin, M. A. Pickard, Y. Song and J. C. Vederas, *J. Am. Chem. Soc.*, 1990, **112**, 4932–4942.
23 B. Pillai, V. A. Moorthie, M. J. van Belkum, S. L. Marcus, M. M. Cherney, C. M. Diaper, J. C. Vederas and M. N. G. James, *J. Mol. Biol.*, 2009, **385**, 580–594.
24 T. Kumagai, Y. Koyama, K. Oda, M. Noda, Y. Matoba and M. Sugiyama, *Antimicrob. Agents Chemother.*, 2010, **54**, 1132–1139.
25 D. Dietrich, M. J. van Belkum and J. C. Vederas, *Org. Biomol. Chem.*, 2012, **10**, 2248–2254.
26 M. P. Malakhov, M. R. Mattern, O. A. Malakhova, M. Drinker, S. D. Weeks and T. R. Butt, *J. Struct. Funct. Genomics*, 2004, **5**, 75–86.
27 R. Assenberg, O. Delmas, S. C. Graham, A. Verma, N. Berrow, D. I. Stuart, R. J. Owens, H. Bourhy and J. M. Grimes, *Acta Crystallogr., Sect. F: Struct. Biol. Cryst. Commun.*, 2008, **64**, 258–262.
28 D. R. Smyth, M. K. Mrozkiewicz, W. J. Mcgrath, P. Listwan and B. Kobe, *Protein Sci.*, 2003, **12**, 1313–1322.
29 C. D. Lee, H. C. Sun, S. M. Hu, C. F. Chiu, A. Homhuan, S. M. Liang, C. H. Leng and T. F. Wang, *Protein Sci.*, 2008, **17**, 1241–1248.
30 M. E. Tanner and S. Miao, *Tetrahedron Lett.*, 1994, **35**, 4073–4076.
31 B. Pillai, M. M. Cherney, C. M. Diaper, A. Sutherland, J. S. Blanchard, J. C. Vederas and M. N. G. James, *Biochem. Biophys. Res. Commun.*, 2007, **363**, 547–553.
32 C. M. Diaper, A. Sutherland, B. Pillai, M. N. G. James, P. Semchuk, J. S. Blanchard and J. C. Vederas, *Org. Biomol. Chem.*, 2005, **3**, 4402–4411.
33 C. W. Koo, A. Sutherland, J. C. Vederas and J. S. Blanchard, *J. Am. Chem. Soc.*, 2000, **122**, 6122–6123.
34 H. Liu, V. R. Pattabiraman and J. C. Vederas, *Org. Lett.*, 2007, **9**, 4211–4214.
35 L. Hor, R. C. J. Dobson, M. T. Downton, J. Wagner, C. A. Hutton and M. A. Perguini, *J. Biol. Chem.*, 2013, **288**, 9238–9248.

